Volume Title
ASP Conference Series, Vol. **Volume Number**
Author
© **Copyright Year** Astronomical Society of the Pacific

arXiv:1607.08844v1 [astro-ph.GA] 29 Jul 2016

The interstellar dust reservoir: SPICA's view on dust production and the interstellar medium in galaxies

F. Kemper[1], R. Zhao-Geisler[2,1], O. C. Jones[3,1] and S. Srinivasan[1]

[1]*Institute of Astronomy and Astrophysics, Academia Sinica, Taiwan*

[2]*National Taiwan Normal University, Taipei, Taiwan*

[3]*Jodrell Bank Centre for Astrophysics, The University of Manchester, UK*

Abstract. Typical galaxies emit about one third of their energy in the infrared. The origin of this emission reprocessed starlight absorbed by interstellar dust grains and reradiated as thermal emission in the infrared. In particularly dusty galaxies, such as starburst galaxies, the fraction of energy emitted in the infrared can be as high as 90%. Dust emission is found to be an excellent tracer of the beginning and end stages of a star's life, where dust is being produced by post-main-sequence stars, subsequently added to the interstellar dust reservoir, and eventually being consumed by star and planet formation. This work reviews the current understanding of the size and properties of this interstellar dust reservoir, by using the Large Magellanic Cloud as an example, and what can be learned about the dust properties and star formation in galaxies from this dust reservoir, using SPICA, building on previous work performed with the *Herschel* and *Spitzer* Space Telescopes, as well as the Infrared Space Observatory.

1. The dust reservoir in galaxies

1.1. Sources and sinks in the Large Magellanic Cloud

The Large Magellanic Cloud (LMC) was imaged using *Spitzer* (SAGE; Meixner et al. 2006) and *Herschel* (HERITAGE; Meixner et al. 2013) using all non-overlapping photometric bands available on these telescopes. The combined SAGE-HERITAGE survey, often referred to as Mega-SAGE, covers the wavelength range from 3.6 to 500 μm. The four *Spitzer*-IRAC bands (3.6–8.0 μm) mainly show circumstellar dust emission from stellar point sources, and extended emission due to polycyclic aromatic hydrocarbons (PAHs), thus forming a good tracer of the production and consumption of dust in post- and pre-main-sequence stars, while the *Spitzer*-MIPS and *Herschel* images show the dust mass in the interstellar medium (ISM). The MIPS 24 μm band represents a transition, while dominated by extended emission due to interstellar dust, extremely dusty point sources are clearly detectable in this band too. It is these point sources with 24-μm detections that dominated the dust production and consumption budget.

Building on a series of previous estimates and methods to determine dust production rates by evolved stars, Riebel et al. (2012) estimate a total dust production rate of $\sim 2.1 \times 10^{-5}$ $M_\odot$ yr^{-1} from the *Spitzer*-IRAC and MIPS data. This rate should be contrasted against the dust mass in the interstellar medium of the LMC, $\sim 10^6$ $M_\odot$ yr^{-1}, derived from the *Herschel* observations Skibba et al. (2012), and the dust consump-

tion in star formation ($\sim 1.9 \times 10^{-3}$; Skibba et al. 2012), assuming a dust-to-gas ratio of 1/200. Taking these numbers at face value, it becomes clear that evolved stars do not produce sufficient dust to replenish the interstellar medium, on the residence time scale of dust in the interstellar medium ($\sim$ 2.5 Gyr; Tielens 1990). Moreover, the much higher dust consumption rate in comparison to the dust production rate even suggests that the dust reservoir in the interstellar medium of the LMC is currently being depleted. This would imply that until fairly recently, the dust production rate was much higher than at the present day, or, alternatively that we are missing a significant source of dust production in this equation.

Three alternatives suggest themselves: **i)** The dust production in supernovae has not been considered in the estimates of dust production by evolved stars in the LMC (e.g. Riebel et al. 2012), due to low number statistics, but estimates suggest that it could be similar to the production by Asymptotic Giant Branch stars (e.g. Whittet 2003). Indeed, Dunne et al. (2003) argued that supernova remnant Cas A has produced 2-4 $M_{\odot}$ of dust, although it has since been shown that the bulk of the dust mass detected is part of a foreground cloud (Krause et al. 2004). From observations of contemporary supernovae in external galaxies, Sugerman et al. (2006) showed that a more realistic number of dust production may lie around $10^{-3} - 10^{-2}$ $M_{\odot}$, although *Herschel* observations of SN 1987A show that it has already produced 0.5 $M_{\odot}$in the first 25 years (Matsuura et al. 2011). **ii)** Dust production in the interstellar medium is efficient, and the source of interstellar dust is not stellar. This has been explored by Zhukovska et al. (2008) and by Jones (2005), and seems to be a viable option. Zhukovska et al. (2008) estimate that the dust production in the interstellar medium in the Solar Neighborhood exceeds the dust production by evolved stars after as little as 1 Gyr. **iii)** Dust production by *extreme* Asymptotic Giant Branch (AGB) stars may be overlooked. Searches for dusty evolved stars rely on classifying point infrared (IRAC, 2MASS) point sources (e.g. Boyer et al. 2011), which are subsequently being fitted against a dust shell model grid to determine the integrated dust production rate (e.g. Sargent et al. 2011; Srinivasan et al. 2011). From this procedure it becomes clear that the dust production is dominated by the reddest objects, the so-called extreme AGB stars. Indeed, Riebel et al. (2012) found that this small number (4%) of extremely red sources account for 75% of the total dust production. This immediately raises the question how many even dustier and redder sources are present, and how they can be detected. With the peak of their spectral energy distributions (SEDs) shifting to even longer wavelengths they can no longer be picked up in the near- or mid-infrared, and far-infrared detections are required. At these wavelengths, the point spread function (PSF) becomes very large, and the point sources need to be bright to stand out over the extended emission due to interstellar dust within the beam. At the distance of the LMC, this is generally not the case, and Boyer et al. (2010) demonstrated that only a small number of known evolved stars in the LMC have counterparts in the *Herschel* data.

1.2. The composition of stellar dust

Including spectroscopy in the analysis of evolved stars enables us to dissect the dust production not only by type of AGB star (carbon-rich or oxygen-rich), but to narrow down the mineralogical components in the freshly produced dust. Although a huge amount of variation exists, and still needs to be further explored, studies like those done by Sargent et al. (2010) and Srinivasan et al. (2010) modeled representative oxygen-rich and carbon-rich AGB star spectra for the LMC, and determined typical

compositions. Combining this with the dust production rate derived from model grid fitting as described above, allows for a determination of the total dust production split out by mineral. It is found that in the LMC, of the dust produced by AGB stars and Red Supergiants, 77 wt.% is in the form of amorphous carbon, 11% in the form of silicon carbide (SiC), 12% in amorphous silicates, and a small fraction of < 1% of the freshly produced dust may be in the form of crystalline silicates (Kemper 2013).

Although most extreme AGB stars turn out to be carbon-rich, the exact composition of dust produced by these stars is hard to determine due to the high optical depth in the circumstellar dust shells. The composition of only the optically thin outer layer can be optimally probed (Speck et al. *in prep.*), so the SiC/amorphous carbon ratio in the vast majority of the dust mass produced by extreme AGB stars remains unknown, although one may assume that it remains constant throughout the mass losing phase of the star.

As stated before, supernovae may be important dust sources too, but so far little is known about the composition of the dust in these environments. One of the few studies that have looked into this is done by Rho et al. (2008), who derived a multi-component composition dominated by amorphous silicates for Cas A in an attempt to fit the main spectral feature at 21 μm.

The interstellar dust of our own Milky Way shows a different composition from what is produced by evolved stars; the majority of the dust is in the form of amorphous silicates, and a smaller fraction in amorphous carbon (Tielens et al. 2005). Only trace amounts of SiC ($\sim 2.6 - 4.2\%$; Min et al. 2007) and crystalline silicates (< 2% Kemper et al. 2004) can be present. The LMC ISM is similar in composition to the Galactic ISM, because the ultraviolet extinction curve between the Milky Way and the LMC is virtually identical, including the relative strength of the 2175 Å bump (Fitzpatrick 1986), meaning similar ratios between carbon-rich and oxygen-rich dust in both galaxies. The discrepancy between ISM dust and stellar dust composition is consistent with the idea that in both galaxies dust formation in denser parts of the ISM itself may dominate the overall dust production, however, there is a contribution from evolved stars that needs to be considered.

2. Observing circumstellar and interstellar dust with SPICA

2.1. The dust reservoir in Local Group galaxies as observed by SPICA

The Mid-Infrared Camera and Spectrograph (MCS) on board of SPICA will operate at 5-38 μm, and this wavelength range will be extended to the near-infrared with the Focal Plane Camera (FPC) which covers the 0.7-5 μm range, providing continuous band coverage from 0.7-38 μm at a spectral resolution $R \approx 5 - 10$. The long wavelength instrument SAFARI will operate at 34-210 μm, and has two modes that are suitable for SED construction: first, the spectroscopic SED mode, with $R \approx 50$, which will allow us to get SEDs from all pixels in a map; and, second, – the more useful option for surveys of the dust budget in galaxies – the photometric mode which covers the SAFARI wavelength range in three broad bands. Thus SPICA uniquely provides a full wavelength coverage from $0.7 - 210$ μm in photometric bands, where for instance *Spitzer* had gaps in the wavelength coverage. In particular the gap between the IRAC-[8.0] and MIPS-[24] band has been hampering the photometric classification of carbon-rich and oxygen-rich AGB stars, as prominent broad spectral features are available in

this range (the 9.7 μm silicate feature, and the 11.3 μm SiC feature). The silicate band can also be used for further constraining the optical depth and thus the mass-loss rate of oxygen-rich AGB stars. The photometric bands available on the suite of instruments on board of SPICA will overcome these problems and can take advantage of the diagnostic power of broad spectral features due to dust, because of the continuous wavelength coverage.

With SPICA it will become possible to do studies of the interstellar dust reservoir and dust injection by evolved stars in galaxies beyond the Magellanic Clouds. Studying external galaxies allows for taking in a global view of the dust reservoir and dust producing stars in the entire galaxy, without having to account for interstellar extinction. Obvious candidates are M31 and M33, the two other spiral galaxies, besides the Milky Way, in the Local Group, at distances of 752 ± 27 kpc (Riess et al. 2012) and 840 kpc (Freedman et al. 1991), respectively. Although M31 is the closest one of the two, it is more inclined, and it will be harder to avoid crowding and confusion, compared to M33.

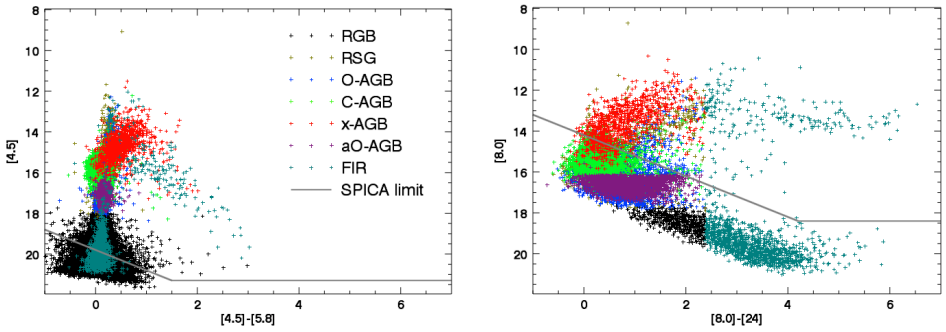

Figure 1. Color-magnitude diagram (CMD) showing different classes of mass-losing evolved stars (SAGE-LMC stars at the distance of M31; only the stars classified by Boyer et al. (2011) are included) and the discovery space of SPICA (gray line). Square brackets denote the brightness in Vega magnitudes at the wavelength enclosed in the brackets. The used *Spitzer* filters match closely with the proposed SPICA-MCS filters. While at shorter mid-IR wavelengths the same stellar populations as for the SAGE LMC with Spitzer can be detected (left), only the stars with a very high mass-loss rate can be found at longer wavelengths (right).

Thus, an exciting possibility is to set up a survey of M31 (or M33) to make an inventory of the stellar content, particularly focused on dusty objects, in a similar fashion as the SAGE-LMC survey (Meixner et al. 2006). We have performed some initial estimates and found that a $1^o \times 3^o$ region encompassing the entirety of M31 can be mapped with 600 pointings using MCS. If we employ 4 filters (two in WFC-L, and two in WFC-S), and do observations in 2 epochs to check for spurious point sources and variability, we find that with the minimum amount of integration time per frame we can perform these observations in $\sim$ 400 hours. The WFC-S and WFC-L modes can be used at the same time, as can the FPC-S instrument, with a slight sky offset. This setup does not cover the full spectral range, but a factor of 5 increase in total time would cover all MCS filters, leading to a project time of $\sim$ 2000 hours for the $1^o \times 3^o$ area covering M31 on the sky. Reductions in integration time can be made again by deciding to cover only half or a quarter of M31, and extrapolating the statistics on the stellar population.

Fig. 1 shows the color-magnitude diagrams (CMD) for the point sources detected in the SAGE-LMC survey, classified by Boyer et al. (2011) into different types of evolved dust producing stars. The bands presented in these diagram are within the MCS wavelength range, and a closely matching MCS equivalent can be identified in the currently proposed filter set. The sample has been placed at the M31 distance and compared with the detection limits of the proposed survey. For the shortest integration times available on MCS, the detection limits for the WFC-S bands are virtually the same for the SAGE-LMC project and the M31 survey proposed in this work, in terms of detectability of the type of object. The detection limit is indicated by a gray line in the each of the panels of Fig. 1. However at longer wavelengths, it turns out that the current detection limit for the proposed survey would not detect the same stellar population in M31 as it did in the SAGE-LMC survey, by at least 2 magnitudes. It appears that the choice of filters with $R \approx 10$ are too narrow to go deep, especially in comparison with MIPS-[24], and perhaps an additional set of 2 or 3 broad band filters for the WFC-L mode would remedy this, making the WFC-L as much of an improvement over MIPS-[24] as that WFC-S has been improved over IRAC-[4.5] and IRAC-[5.8].

2.2. Spectroscopy with the Mid-infrared Camera and Spectrograph (MCS)

The currently proposed MCS instrument includes two spectroscopic modes: the High Resolution Spectrograph (HRS-L), which will operate at 12-18 μm, with $R \approx 20,000 - 30,0000$. and the Medium Resolution Spectrograph, which will operate at 12.2-23.0 μm, with $R \approx 2000$ (MRS-S) and at 23.0-37.5 μm, with $R \approx 1000$ (MRS-L). For the purpose of studying solid state features, the spectral resolution offered by the MRS is sufficient to do a detailed analysis of the mineralogy. Unfortunately, the wavelength coverage of the MRS mode does not include a number of important spectral features:

- The Si-O stretching mode in amorphous and crystalline silicates around 9.7 μm.
- Features due to polycyclic aromatic hydrocarbons (PAHs) from 6-12 μm.
- Two out of the four identified bands of C_{60}, namely those at 7.0 and 8.5 μm.
- Ice features at 4.2 μm due to CO_2; 6.0 μm due to H_2O and 6.8 μm due to a still unidentified carrier
- Absorption lines from C_2H_2 and other molecules related to dust formation.
- Spectral features due to alumina, oxides and quartz.
- The 11.3 μm feature due to SiC.

The wavelength range shortward of 12.2 μm is covered by a grism in WFC-S, with an intended spectral resolution of $R \approx 50$. While this may, in some cases, be sufficient to detect the presence of these features, it is not possible to do any compositional analysis, such as for instance the crystalline fraction of silicates, which is revealed by the shape of the resonance. For such an analysis, the observations should match the spectral resolution of laboratory data, which is typically taken at R of a few hundred. Moreover, the detection of narrow features, such as the C_2H_2 absorption lines, or the C_{60} narrow emission bands will be virtually impossible at $R \approx 50$. Thus we recommend the insertion of a $R \approx 200$ grism in the WFC-S filter wheel, with a wavelength coverage of

5.0-12.2 μm. Perhaps this may have to be divided over two grisms, to avoid problems with the dispersion.

There are a number of other interesting dust and ice resonances that are included in the MRS wavelength coverage. Here we highlight a few examples, to illustrate the discovery space that can be further explored with the MRS mode on the MCS.

First, carbon dioxide (CO_2) in its pure form has a double-peaked resonance around 15.2 μm (Ehrenfreund et al. 1999). This double-peaked structure becomes less pronounced or disappears altogether when the a-polar CO_2 ice is embedded in polar H_2O-rich ices. The depth of the trough between the two peaks can provide information about the amount of thermal processing, and thus about the degree of separation between the two ice components (CO_2 and H_2O) in embedded objects, such as the envelopes of young stars. Moreover, the 15.2 μm resonance due to CO_2 develops a shoulder on the red side and gradually shifts towards longer wavelengths overall, when it is mixed with methanol (CH_3OH) (Ehrenfreund et al. 1999). For instance Zasowski et al. (2009) have shown that studying the exact shape of the 15.2 micron absorption feature due to CO_2 at a resolution of $R \approx 600$ can indeed be used as a tool to determine the composition of the ice mixture, and establish the degree of processing for different objects. Specifically, they find that in a sample of 16 Class I/II objects the typical ice composition is dominated by water ice, with ~12% CO_2, and up to ~10% of methanol ice. The ice absorption features at shorter wavelengths (6-12 μm) also provided constraints on further ice components.

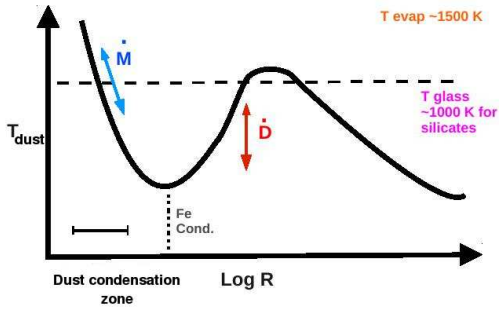

Figure 2. Schematic of the dust temperature profile as a function of distance to the central star. The dotted line indicates the level of the glass temperature, above which silicates can become crystalline. Depending on the gas density (defined by the mass-loss rate $\dot{M}$), dust condensation starts at a different distance from the star, indicated by the blue arrow. This decides whether the silicates are formed crystalline or amorphous. As the grains move outwards, the temperature drops until it is low enough for iron to condense, which cause the UV/optical opacity to increase, and thus the grain temperature can be raised above the glass temperature (annealing). Figure adapted from Sogawa & Kozasa (1999).

A second topic of great interest in the wavelength range covered by MRS is the thermal processing of silicates. Silicates observed in the interstellar medium are probably not of stoichiometric composition, and show many lattice defects, often referred to in the astromineralogy community as being *amorphous* (see e.g. Kemper et al. 2004). These amorphous silicates only show broad resonances due to the Si-O stretching mode at 9.7 μm, and the O-Si-O bending mode at 18 μm. However, when silicates are exposed

to temperatures above the glass temperature ($\sim$ 1000 K), annealing occurs, and the silicates may become crystalline. The spectral signature of crystalline silicates is quite different, and show a wealth of narrower resonances due to increased regularity in the lattice (See Fig. 1 of Molster & Kemper 2005). Although it is known that an increased level of crystallinity is due to exposure of the silicates to high temperatures, it is not clear whether this is due to annealing of amorphous silicates, as for instance modeled by Sogawa & Kozasa (1999), or from direct condensation in the gas phase (See Fig. 2). Recently, Jones et al. (2012) used a sample of oxygen-rich AGB stars from the Milky Way, the LMC and the SMC, representing three different metallicities, to show that the transition between sources showing crystalline silicates or sources without them, is much sharper for the dust mass-loss rate, than for the gas mass-loss rate, suggesting that annealing (heating of amorphous silicates) is the dominant crystallization mechanism.

Finally, a recent exciting discovery is the detection of interstellar C_{60} (Cami et al. 2010), by its infrared resonances at 7.0, 8.5, 17.4 and 18.89 μm. The line strengths in these four bands provide clues to the excitation and formation mechanisms of this enigmatic molecule (Bernard-Salas et al. 2012; Micelotta et al. 2012), and its chemical closeness to PAHs may also help understand the formation of these pre-biotic molecules.

2.3. Spectroscopy with SAFARI

With the SAFARI instrument, the 38-55 μm range is spectrally accessible for the first time in well over a decade, after the Infrared Space Observatory (ISO) was able to do this. SAFARI will operate at 34-210 μm, with different spectral resolutions, namely $R \approx 50$, $R \approx 500$ and $R \approx 2000$. Especially $R \approx 500$ is very suitable for mineralogical studies in interstellar and circumstellar environments, and here we highlight three of possible research areas that can be further explored.

First, in 2002, the presence of carbonates in two planetary nebulae was discovered using the features of dolomite at 62 μm and calcite at 92 μm (Kemper et al. 2002). This was the first extrasolar detection of these minerals, and their discovery in this non-parent-body environment suggest a formation path in the absence of liquid water. An archival search of the spectra of young stellar objects observed with ISO-LWS revealed a further 17 detections of carbonates (Chiavassa et al. 2005), but additional detections with *Herschel* have not been reported yet, due to the difficulty of detecting broad bands in the PACS spectroscopy. With SAFARI a systematic survey into the occurrence of these resonances can be performed.

Second, in the SAFARI wavelength range, two water ice features, at 43 and 63 μm may appear in emission. Previously, these emission features have been observed towards YSOs (Malfait et al. 1999) and post-AGB stars (Hoogzaad et al. 2002) with ISO-LWS. Water ice is less volatile than CO_2 ice, sticking to dust grains at higher temperatures, and the ratio between the CO_2/H_2O mass fractions informs us about the amount of thermal processing of the ice. Moreover, the shape and appearance of the 43 and 63 μm resonances depend on the lattice structure of the water ice, providing further information on the formation and processing history.

Finally, SAFARI will offer a further opportunity to study the 69 μm resonance due to forsterite, initially discovered with ISO-LWS. This crystalline silicate feature is very sensitive in peak position to both composition (Fe-content) and dust temperature (Molster et al. 2002), and provides a valuable constraint to dust models based on crystalline silicate detections at shorter wavelengths. This feature is narrow enough that

it could reliably be detected with *Herschel*-PACS (Sturm et al. 2010), but so far it has only been analyzed for a handful of objects, allowing for further discovery space to be filled in by SAFARI observations.

Acknowledgments. FK wishes to acknowledge support from the National Science Council under grant number NSC100-2112-M-001-023-MY3.

References

Bernard-Salas, J., Cami, J., Peeters, E., Jones, A. P., Micelotta, E. R., & Groenewegen, M. A. T. 2012, ApJ, 757, 41. 1207.5794

Boyer, M. L., Sargent, B., van Loon, J. T., Srinivasan, S., Clayton, G. C., Kemper, F., Smith, L. J., Matsuura, M., Woods, P. M., Marengo, M., Meixner, M., Engelbracht, C., Gordon, K. D., Hony, S., Indebetouw, R., Misselt, K., Okumura, K., Panuzzo, P., Riebel, D., Roman-Duval, J., Sauvage, M., & Sloan, G. C. 2010, A&A, 518, L142. 1005.5167

Boyer, M. L., Srinivasan, S., van Loon, J. T., McDonald, I., Meixner, M., Zaritsky, D., Gordon, K. D., Kemper, F., Babler, B., Block, M., Bracker, S., Engelbracht, C. W., Hora, J., Indebetouw, R., Meade, M., Misselt, K., Robitaille, T., Sewiło, M., Shiao, B., & Whitney, B. 2011, AJ, 142, 103. 1106.5026

Cami, J., Bernard-Salas, J., Peeters, E., & Malek, S. E. 2010, Science, 329, 1180

Chiavassa, A., Ceccarelli, C., Tielens, A. G. G. M., Caux, E., & Maret, S. 2005, A&A, 432, 547

Dunne, L., Eales, S., Ivison, R., Morgan, H., & Edmunds, M. 2003, Nat, 424, 285. astro-ph/0307320

Ehrenfreund, P., Kerkhof, O., Schutte, W. A., Boogert, A. C. A., Gerakines, P. A., Dartois, E., D'Hendecourt, L., Tielens, A. G. G. M., van Dishoeck, E. F., & Whittet, D. C. B. 1999, A&A, 350, 240

Fitzpatrick, E. L. 1986, AJ, 92, 1068

Freedman, W. L., Wilson, C. D., & Madore, B. F. 1991, ApJ, 372, 455

Hoogzaad, S. N., Molster, F. J., Dominik, C., Waters, L. B. F. M., Barlow, M. J., & de Koter, A. 2002, A&A, 389, 547

Jones, A. P. 2005, in ESA Special Publication, edited by A. Wilson, vol. 577 of ESA Special Publication, 239

Jones, O. C., Kemper, F., Sargent, B. A., McDonald, I., Gielen, C., Woods, P. M., Sloan, G. C., Boyer, M. L., Zijlstra, A. A., Clayton, G. C., Kraemer, K. E., Srinivasan, S., & Ruffle, P. M. E. 2012, MNRAS, 427, 3209. 1208.4950

Kemper, F. 2013, Earth, Planets and Space, 65, 223

Kemper, F., Jäger, C., Waters, L. B. F. M., Henning, T., Molster, F. J., Barlow, M. J., Lim, T., & de Koter, A. 2002, Nature, 415, 295

Kemper, F., Vriend, W. J., & Tielens, A. G. G. M. 2004, ApJ, 609, 826. astro-ph/0403609

Krause, O., Birkmann, S. M., Rieke, G. H., Lemke, D., Klaas, U., Hines, D. C., & Gordon, K. D. 2004, Nat, 432, 596. astro-ph/0412092

Malfait, K., Waelkens, C., Bouwman, J., de Koter, A., & Waters, L. B. F. M. 1999, A&A, 345, 181

Matsuura, M., Dwek, E., Meixner, M., Otsuka, M., Babler, B., Barlow, M. J., Roman-Duval, J., Engelbracht, C., Sandstrom, K., Lakićević, M., van Loon, J. T., Sonneborn, G., Clayton, G. C., Long, K. S., Lundqvist, P., Nozawa, T., Gordon, K. D., Hony, S., Panuzzo, P., Okumura, K., Misselt, K. A., Montiel, E., & Sauvage, M. 2011, Science, 333, 1258. 1107.1477

Meixner, M., Gordon, K. D., Indebetouw, R., Hora, J. L., Whitney, B., Blum, R., Reach, W., Bernard, J.-P., Meade, M., Babler, B., Engelbracht, C. W., For, B.-Q., Misselt, K., Vijh, U., Leitherer, C., Cohen, M., Churchwell, E. B., Boulanger, F., Frogel, J. A., Fukui, Y., Gallagher, J., Gorjian, V., Harris, J., Kelly, D., Kawamura, A., Kim, S., Latter, W. B., Madden, S., Markwick-Kemper, C., Mizuno, A., Mizuno, N., Mould, J., Nota, A., Oey, M. S., Olsen, K., Onishi, T., Paladini, R., Panagia, N., Perez-Gonzalez, P., Shibai, H.,

Sato, S., Smith, L., Staveley-Smith, L., Tielens, A. G. G. M., Ueta, T., van Dyk, S., Volk, K., Werner, M., & Zaritsky, D. 2006, AJ, 132, 2268. astro-ph/0606356

Meixner, M., Panuzzo, P., Roman-Duval, J., Engelbracht, C., Babler, B., Seale, J., Hony, S., Montiel, E., Sauvage, M., Gordon, K., Misselt, K., Okumura, K., Chanial, P., Beck, T., Bernard, J.-P., Bolatto, A., Bot, C., Boyer, M. L., Carlson, L. R., Clayton, G. C., Chen, C.-H. R., Cormier, D., Fukui, Y., Galametz, M., Galliano, F., Hora, J. L., Hughes, A., Indebetouw, R., Israel, F. P., Kawamura, A., Kemper, F., Kim, S., Kwon, E., Lebouteiller, V., Li, A., Long, K. S., Madden, S. C., Matsuura, M., Muller, E., Oliveira, J. M., Onishi, T., Otsuka, M., Paradis, D., Poglitsch, A., Reach, W. T., Robitaille, T. P., Rubio, M., Sargent, B., Sewiło, M., Skibba, R., Smith, L. J., Srinivasan, S., Tielens, A. G. G. M., van Loon, J. T., & Whitney, B. 2013, AJ, 146, 62

Micelotta, E. R., Jones, A. P., Cami, J., Peeters, E., Bernard-Salas, J., & Fanchini, G. 2012, ApJ, 761, 35. 1207.5817

Min, M., Waters, L. B. F. M., de Koter, A., Hovenier, J. W., Keller, L. P., & Markwick-Kemper, F. 2007, A&A, 462, 667. astro-ph/0611329

Molster, F., & Kemper, C. 2005, Space Sci. Rev., 119, 3

Molster, F. J., Waters, L. B. F. M., Tielens, A. G. G. M., Koike, C., & Chihara, H. 2002, A&A, 382, 241. astro-ph/0201305

Rho, J., Kozasa, T., Reach, W. T., Smith, J. D., Rudnick, L., DeLaney, T., Ennis, J. A., Gomez, H., & Tappe, A. 2008, ApJ, 673, 271. 0709.2880

Riebel, D., Srinivasan, S., Sargent, B., & Meixner, M. 2012, ApJ, 753, 71. 1205.0280

Riess, A. G., Fliri, J., & Valls-Gabaud, D. 2012, ApJ, 745, 156

Sargent, B. A., Srinivasan, S., & Meixner, M. 2011, ApJ, 728, 93. 1407.8452

Sargent, B. A., Srinivasan, S., Meixner, M., Kemper, F., Tielens, A. G. G. M., Speck, A. K., Matsuura, M., Bernard, J.-P., Hony, S., Gordon, K. D., Indebetouw, R., Marengo, M., Sloan, G. C., & Woods, P. M. 2010, ApJ, 716, 878. 1407.6996

Skibba, R. A., Engelbracht, C. W., Aniano, G., Babler, B., Bernard, J.-P., Bot, C., Carlson, L. R., Galametz, M., Galliano, F., Gordon, K., Hony, S., Israel, F., Lebouteiller, V., Li, A., Madden, S., Meixner, M., Misselt, K., Montiel, E., Okumura, K., Panuzzo, P., Paradis, D., Roman-Duval, J., Rubio, M., Sauvage, M., Seale, J., Srinivasan, S., & van Loon, J. T. 2012, ApJ, 761, 42. 1210.7812

Sogawa, H., & Kozasa, T. 1999, ApJ, 516, L33

Srinivasan, S., Sargent, B. A., Matsuura, M., Meixner, M., Kemper, F., Tielens, A. G. G. M., Volk, K., Speck, A. K., Woods, P. M., Gordon, K., Marengo, M., & Sloan, G. C. 2010, A&A, 524, A49. 1009.2681

Srinivasan, S., Sargent, B. A., & Meixner, M. 2011, A&A, 532, A54. 1106.3256

Sturm, B., Bouwman, J., Henning, T., Evans, N. J., Acke, B., Mulders, G. D., Waters, L. B. F. M., van Dishoeck, E. F., Meeus, G., Green, J. D., Augereau, J. C., Olofsson, J., Salyk, C., Najita, J., Herczeg, G. J., van Kempen, T. A., Kristensen, L. E., Dominik, C., Carr, J. S., Waelkens, C., Bergin, E., Blake, G. A., Brown, J. M., Chen, J.-H., Cieza, L., Dunham, M. M., Glassgold, A., Güdel, M., Harvey, P. M., Hogerheijde, M. R., Jaffe, D., Jørgensen, J. K., Kim, H. J., Knez, C., Lacy, J. H., Lee, J.-E., Maret, S., Meijerink, R., Merín, B., Mundy, L., Pontoppidan, K. M., Visser, R., & Yıldız, U. A. 2010, A&A, 518, L129. 1005.3472

Sugerman, B. E. K., Ercolano, B., Barlow, M. J., Tielens, A. G. G. M., Clayton, G. C., Zijlstra, A. A., Meixner, M., Speck, A., Gledhill, T. M., Panagia, N., Cohen, M., Gordon, K. D., Meyer, M., Fabbri, J., Bowey, J. E., Welch, D. L., Regan, M. W., & Kennicutt, R. C. 2006, Science, 313, 196. astro-ph/0606132

Tielens, A. G. G. M. 1990, in From Miras to Planetary Nebulae: which path for stellar evolution?, edited by M. O. Mennessier, & A. Omont, 186

Tielens, A. G. G. M., Waters, L. B. F. M., & Bernatowicz, T. J. 2005, in Chondrites and the Protoplanetary Disk, edited by A. N. Krot, E. R. D. Scott, & B. Reipurth (San Francisco: Astron. Soc. Pac.), vol. 341 of ASP Conf. Ser., 605

Whittet, D. C. B. 2003, Dust in the galactic environment (London: Institute of Physics Publishing)

Zasowski, G., Kemper, F., Watson, D. M., Furlan, E., Bohac, C. J., Hull, C., & Green, J. D. 2009, ApJ, 694, 459. 0712.2458
Zhukovska, S., Gail, H.-P., & Trieloff, M. 2008, A&A, 479, 453. 0706.1155